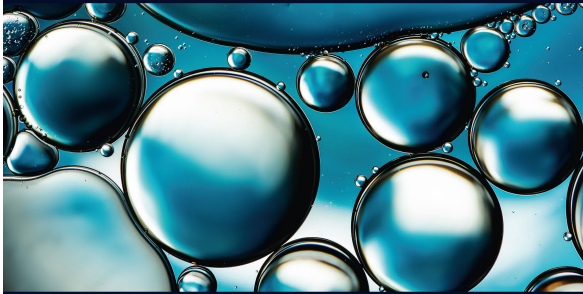




Christina Kallendorf (Autor)

An Eulerian Discontinuous Galerkin Method for the Numerical Simulation of Interfacial Transport



**An Eulerian Discontinuous Galerkin
Method for the Numerical Simulation
of Interfacial Transport**

Christina Kallendorf



Cuvillier Verlag Göttingen
Internationaler wissenschaftlicher Fachverlag

<https://cuvillier.de/de/shop/publications/7480>

Copyright:

Cuvillier Verlag, Inhaberin Annette Jentsch-Cuvillier, Nonnenstieg 8, 37075 Göttingen,
Germany

Telefon: +49 (0)551 54724-0, E-Mail: info@cuvillier.de, Website: <https://cuvillier.de>

1 Introduction

1.1 Motivation

In various applications, it is important to model, simulate and compute processes on surfaces, curves or on more general submanifolds. Most of these processes are governed by partial differential equations (PDEs) on surfaces, or on submanifolds, respectively. Depending on the application, the problem domain is either steady, or deforming, or moving and deforming at the same time. These distinct cases imply an increasing complexity of the problem. Areas of interest range from fluid mechanics, bio-chemistry and medical imaging to image processing.

For example, in image processing, surface differential equations on steady surfaces are involved when smoothing and regularizing images (Diewald, Preußer, Rumpf, and Strzodka, 2001). Denoising (Bertalmío, Cheng, Osher, and Sapiro, 2001) as well as deblurring (Cheng, 2000) of images is achieved by solving surface diffusion equations, for instance, in brain imaging (Mémoli, Sapiro, and Thompson, 2004).

In biochemistry, the interaction of pairs of chemicals, called morphogenes, in the epithelial, i.e. outer, layer of growing organisms is modelled by reaction-diffusion equations on the organisms' surface (Leung and Berzins, 2003a). Morphogenes have been used in modelling spatial pattern formation and the regeneration of body cells such as receptor cells in the eye of a *Drosophila* (Koch and Meinhardt, 1994). Coat markings of mammals as well as the formation of skeletal pattern are assigned to morphogenes (Maini, Painter, and Nguyen Phong Chau, 1997). These morphogenesis processes are governed by differential equations on *deforming* surfaces.

In fluid mechanics, the transport of mass, energy or momentum on phase interfaces is a topic of increasing importance. Here, interfacial transport is modelled by PDEs on the phase interface and therefore, on *moving* and *deforming* interfaces. In particular, it is often inevitable to examine the transport of surface active substances on the moving interface, such as emulsifiers or detergents. For their surface active behavior, these compounds are known as surface active agents, or shortly *surfactants* (Schramm, 2000). The transport of these substances on two-phase interfaces is governed by convection-diffusion equation defined on evolving surfaces. These surfaces may change rapidly with respect to geometry or topology.



Because their structure includes both a part which has affinity to nonpolar media and one part that has an affinity to polar media, surfactants adsorb at interfaces that separate media of different polarity. During adsorption, the surfactant molecules form a monolayer on the interface between the immiscible phases, destroying the cohesive forces between the polar and non-polar molecules and replacing them. While the hydrophilic head of the adsorbed surfactant molecule orients itself towards the polar phase, the hydrophobic tail lies either flat on the interface, or aligns itself to the less polar liquid (Gecol, 2007), if the interface is sufficiently occupied. As a consequence of the adsorption process, most types of surfactants reduce the interfacial free energy, i.e. the surface tension (Tricot, 1997a). This implies that the surface tension of a surfactant covered interface is lower than the one of a clean interface. Furthermore, the interfacial tension is comparatively lower in interfacial regions of high surfactant concentration. When the surfactant is not uniformly distributed, a Marangoni force is introduced by the gradient that exists in surfactant concentration. This Marangoni force is directed from regions of high surfactant concentration to regions of low surfactant concentration along the interface (Kas-Danouche, Papageorgiou, and Siegel, 2004).

Numerous industrial processes that involve two-phase or free surface flows require controlling mechanisms of the surface tension. For this purpose, surfactants are usually added to either of the phases.

Silicone surfactants are used as stabilizing agents for polyetherane foam by reducing interfacial tension and, consequently, promoting the formation of a coherent interfacial film (Snow, Pernisz, and Braun, 2006). They function as stabilizer of foams, for instance, in enhanced oil recovery or drilling operations.

Surfactants are used to control the formation of small droplets in industrial emulsification processes by lowering the surface tension, and hence facilitating the droplet breakup and preventing coalescence (Janssen, Boon, and Agterof, 1994; Eggleton, Tsai, and Stebe, 2001). Surfactants are commonly added to stabilize emulsions, i.e. mixtures of two or more immiscible fluids, such as oil and water. Emulsions are present not only in food, cosmetic and pharmaceutical products, but they are also frequently applied in technical processes. For instance, emulsions are used as cooling lubricants in order to minimize both frictional effects and temperature during machining processes, for instance, in metal fabrication (Doll and Sharma, 2011). Emulsified fuels, where water droplets are dispersed in the fuel and stabilized by a surfactant additive, are used in automotive technology in order to minimize emissions. For example, water in diesel dispersions have been investigated as direct fuel substitutes that can be utilized with little or no modifications in existing diesel engines by Nadeem, Rangkuti, Anuar, Haq, Tan, and Shah (2006). They were reported to significantly reduce the emissions of NO_x , CO , SO_x as well as particle matter.

Coating forms an important aspect of numerous industrial manufacturing processes in order to protect, functionalize and lubricate surfaces. Surfactants are often employed as additives to facilitate coating processes by reducing the surface tension (Tricot, 1997b). At the same time, several processes involve coating liquids that are surfactant



solutions, and surface and bulk rheology of these solutions naturally impacts the coating properties.

From the numerical perspective, evolving interfacial physical quantities along a moving deformable surface is a highly challenging task. The surface differential operators involved require a thoughtful approximation that is distinct from the available discretizations of standard differential operators. Depending on the method applied, tracking or capturing an interface also requires great expertise. In most research works a Lagrangian grid is used to track the phase interface and employed to discretize interfacial equations, implying that these equations are only solved on the interface, see e.g. Ceniceros (2003), James and Lowengrub (2004), Kruijt-Stegeman, van de Vosse, and Meijer (2004), Lai, Tseng, and Huang (2008), Lee and Pozrikidis (2006), Muradoglu and Tryggvason (2008) or Zhang, Eckmann, and Ayyaswamy (2006).

In the present work, a numerical framework for solving interfacial convection-diffusion problems is established. In contrast to these traditional approaches, the method presented here does **not** treat interfacial transport problems by establishing a Lagrangian, i.e. interfacial grid, but instead, it is founded on maintaining the Eulerian grid. Up to now, considerably fewer works on numerical simulations of interfacial equations are based on such an Eulerian approach. Several limited examples are given by Bertalmío, Cheng, Osher, and Sapiro (2001), Greer (2006), Greer, Bertozzi, and Sapiro (2006), Burger (2009) as well as Dziuk and Elliott (2009) for various interfacial differential equations. Especially when the a surface moves and deforms quickly, as in the case of a fluidic interface, an Eulerian representation of the surface differentials has favorable properties. Beyond, the method can be easily combined with an interface capturing technique that presumes an implicit representation of the interface.

For this purpose, the Discontinuous Galerkin (DG) method is employed, which incorporates favorable features of both Finite Element (FE) and Finite Volume (FV) methods. The DG method has become increasingly popular in the past decades, as it combines polynomial approximations of arbitrary order with the use of numerical fluxes to approximate integrals over the cell boundaries. Consequently, the DG approach is highly convenient for hyperbolic problems. At the same time, it is flexible with respect to the domain's geometry and achieves $\mathcal{O}(h^p)$ order of convergence. Importantly, the use of numerical fluxes establishes a local block structure of the discretization, which supports parallel computing, and allows to incorporate boundary conditions easily. The treatment of surface convection-diffusion equations by the DG method highly benefits from these features, and to the author's knowledge, it is the first published work that pursues an Eulerian approach for resolving surface differential operators in the context of a DG method.

A parallelized and modular package for the numerical simulation of interfacial transport problems is designed. The library, developed in C#, discretizes both interfacial convection and convection-diffusion equations by a DG method, and is integrated in the existing software framework *BoSSS* initiated by Kummer (2012). Here, the surface convection-diffusion equation is extended into the underlying three-dimensional space by identifying the surface gradient with the projection of the standard gradient to

its tangential part. In this way, the interfacial transport problem can be discretized based on the existent Eulerian grid, at the same time admitting an implicit interface representation as the zero-isocontour of a Level Set function. In contrast to the Lagrangian approach, this Eulerian approach is highly suitable for moving and deforming interfaces and allows for an accurate resolution of the interface.

1.2 Thesis Outline

The present work is structured as follows.

The surface differential equations under consideration focus on the general case of interfacial transport in fluid mechanical applications. For this reason, in chapter 2, starting from the standard postulates of continuum mechanics, the derivation of local mass balance laws for the bulk phases and for the phase interface for some arbitrary physical quantity are provided, following Wang and Oberlack, 2011. The resulting equations are then employed to derive the equations of the physical model under consideration, i.e. the Navier–Stokes equations for two phases, including interfacial jump conditions, and the interfacial convection–diffusion equation describing material transport at a two–phase interface.

Chapter 3 gives a comprehensive overview of existing numerical research on surface and interfacial transport. Available methods are classified as traditional *Lagrangian approaches*, where the submanifold itself is resolved by a Lagrangian grid, or as *Eulerian approaches*, where the interfacial problem is extended into the underlying three–dimensional domain and discretized on basis of the given Eulerian grid. Special attention is paid to existing works dealing with interfacial transport in fluid mechanical applications. In this context, the method selected for the treating the interfacial equations highly depends on the approach employed for tracking or capturing the interface. Therefore, numerical methods that are available for representing the phase interphase are additionally outlined in chapter 3.

The solver developed within the context of this work is based on a Discontinuous Galerkin (DG) discretization of the transport problem. For this reason, the fundamentals of the DG method are explained in chapter 4 with a particular focus on the PDEs relevant to the subsequent work. Its characteristic features are underlined, pointing out to the motivation for founding the subsequent approximations on a DG scheme. Against this background, chapter 4 further motivates the design of the method presented, incorporating an interface capturing approach by a Level Set function and an Eulerian approach for resolving the surface differentials.

In the Eulerian formulation, however, the conserved form of the interfacial balance law is destroyed by the extension of the interfacial differential equation to the three–dimensional domain. This fact has been identified as an obstacle at the initial project phase. From the viewpoint of numerical accuracy, the conserved form of a differential equation is always favorable to reduce numerical errors and preserve the quantity numerically. In chapter 5, infinite sets of conservation laws have been discovered



by using the direct construction method, i.e. by applying local conservation law multipliers (Kallendorf, Cheviakov, Oberlack, and Wang, 2012). These conserved forms constitute a well-suited basis for discretizing the interfacial transport equation by a DG scheme, while maintaining an implicit representation of the interface. The obtained results are also applicable to the construction of more general balance laws for other excess surface physical quantities. The system of governing equations is subsequently rewritten in a fully conserved form in the three-dimensional domain.

In chapter 6, general exact solutions to the interfacial transport of a solute on the spherical surface with both convective and diffusive terms are developed (Kallendorf, Fath, Oberlack, and Wang, 2015). The transport of insoluble surfactant in a Stokes flow setting is investigated, where a spherical shaped inner phase is dispersed in an outer phase. The model is simplified by assuming that the impact of the surfactant on surface tension is negligible. Its investigation has been motivated by the lack of exact solutions to the interfacial transport problem. The general solutions derived involve Heun's confluent functions, and for the steady case, it is shown that these solutions collapse to a simple exponential form. Furthermore, for the purely diffusive problem, exact solutions are constructed using Legendre polynomials.

The embedded interfacial transport problem is discretized on a small subdomain of the original domain only, which is given by a Narrow Band tube of few cells thickness around the interface. As this narrow band changes position and structure in accordance with the interface, it is not created as an independent physical grid, but rather induced from the full grid through selective storage allocation and extraction of the relevant entries, or coordinates, respectively. Chapter 7 describes how such a coordinate based Narrow Band is implemented within the software framework `BOSSS` (Kummer, 2012). Furthermore, a method for extending values to newly acquired cells of this subdomain is developed and analysed in chapter 8. This tool, which is based on employing a pseudo-timestepping scheme, is essential when discretizing problems on a dynamically moving Narrow Band.

Chapter 8 describes the Eulerian DG scheme that is established in the present work for discretizing interfacial transport equations. This implementation is based on simplest forms of the conservation laws that have been developed in chapter 5. The convection-diffusion equation is discretized by a simple operator splitting scheme, which motivates to solve the purely convective and the purely diffusive parts of the conserved form independently. Computational examples of all of the three forms of surface transport equation are developed and solved for both two- and three-dimensional underlying domains. Based on exact solutions to the two-dimensional examples, a study of convergence is presented, where the purely convective equation, both on a steady and on a moving surface, as well as the purely diffusive equation on a steady surface are considered. Illustrations of sample problems are provided for problems of all mentioned complexities, i.e. for steady, but complex, moving as well as moving and deforming surfaces.



To conclude, chapter 9 summarizes the results achieved within the context of the present thesis. This chapter concludes with an outlook of further improvements and ideas for continued research.

2 Equations of the Physical Model

2.1 Transport Equations in Two-Phase Flow

In this section, starting from the standard postulates of continuum mechanics, local mass balance laws for the bulk phases and for the phase interface are derived for some arbitrary physical quantity. The derivation presented here is adopted from Wang and Oberlack (2011), who established, in addition to the classical mass balance laws for the bulks in a three-phase setting, local mass balance laws for phase interfaces and contact lines. The resulting equations are then employed to derive the equations of the physical model under consideration, i.e. the Navier – Stokes equations for two phases, including interfacial jump conditions, and the material transport equations at a two-phase interface and in the bulks.

2.1.1 Mass Balance Laws in a Two-Phase Setting

Let Γ denote a physical variable characterizing a partial aspect of a state of a body at time t . A material domain $\Omega(t)$ of the body under consideration is chosen with respect to which the physical variable is evaluated. For this purpose, a setting with two immiscible phases is assumed, considering a material domain Ω which is decomposed into two disjoint subdomains $\mathfrak{B}^{(1)}$ and $\mathfrak{B}^{(2)}$ occupied by the distinct phases. The two phases are separated by a curved surface \mathfrak{S} , the phase interface, which can be identified with a two-dimensional, moving, orientable and mathematically singular surface in the three-dimensional Euclidian space. This surface is singular in the sense that a vanishing interface thickness is considered, across which the physical quantities may be discontinuous.

In fact, in multiphase systems, an interface is rather given by a thin transition layer of only few molecular layers thickness, across which physical quantities, such as mass or momentum, change smoothly but rapidly. But as the thickness of this interfacial transition zone ranges at the nanometer scale, the interface is infinitely thin as compared to the dimensions of the adjacent bulks and can be considered as a two-dimensional continuum, with its own material properties, for instance, surface tension.

The material domain Ω is bounded by an outer boundary $\partial\Omega = \partial\mathfrak{B}^{(1)} \cup \partial\mathfrak{B}^{(2)} \cup \mathfrak{C}$ in Lagrangian representation, where the curve \mathfrak{C} denotes the intersection of the interface \mathfrak{S} with the domain's boundary $\partial\Omega$. As depicted in figure 2.1, n denotes the outward

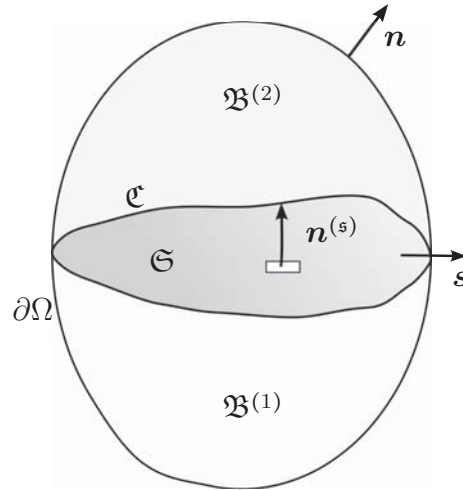


Figure 2.1: Control volume that is occupied by two phases, separated by an interface.

unit normal vector of $\partial\Omega$ and $\mathbf{n}^{(s)}$ the unit normal of the interface \mathfrak{S} , pointing from $\mathfrak{B}^{(1)}$ into $\mathfrak{B}^{(2)}$. In addition, the unit normal \mathbf{s} to the curve \mathfrak{C} , which is tangent to the interface and oriented outward from the system, is needed in the following derivations.

Denoting the total time derivative by $\frac{d}{dt}$, the time rate of change of the physical variable Γ of the body per unit time can be decomposed into

$$\frac{d\Gamma}{dt} = F + P + S, \quad (2.1)$$

distinguishing the flux F of the variable from outside into the body through the surface $\partial\Omega$, its production P within the domain as well as its supply S , or source by action, at a distance from outside of the body. The physical variable can be specified by means of densities $\gamma^{(i)}$, in each subdomain $\mathfrak{B}^{(i)}$, $i = 1, 2$, and density $\gamma^{(s)}$, on the interface \mathfrak{S} , respectively, in Eulerian representation, i.e.

$$\Gamma = \sum_{i=1}^2 \int_{\mathfrak{B}^{(i)}} \gamma^{(i)} dv + \int_{\mathfrak{S}} \gamma^{(s)} da. \quad (2.2)$$

On the interface, densities of the respective surface excess amounts are employed. The surface excess $N_l^{(s)}$ of a component l corresponds to the difference between its actual amount present in the real system, and its amount in a reference system if its concentration within the adjacent bulks is extended to a chosen geometrical dividing surface (Mitropoulos, 2008). The dividing surface, i.e. singular interface, is usually located where the surface excess of the solvent is zero, as depicted in figure 2.2. Likewise, the terms on the right hand side can be expressed in integral form employing

- the non-convective bulk flux densities of Γ (per unit surface area), $\phi^{(i)}$ ($i = 1, 2$), through the material outer surfaces $\partial\mathfrak{B}^{(i)}$ of the bulk phases $\mathfrak{B}^{(i)}$,
- the non-convective surface flux density of Γ (per unit line length), $\phi^{(s)}$, through the outer boundary curve \mathfrak{C} of the phase interface \mathfrak{S} ,

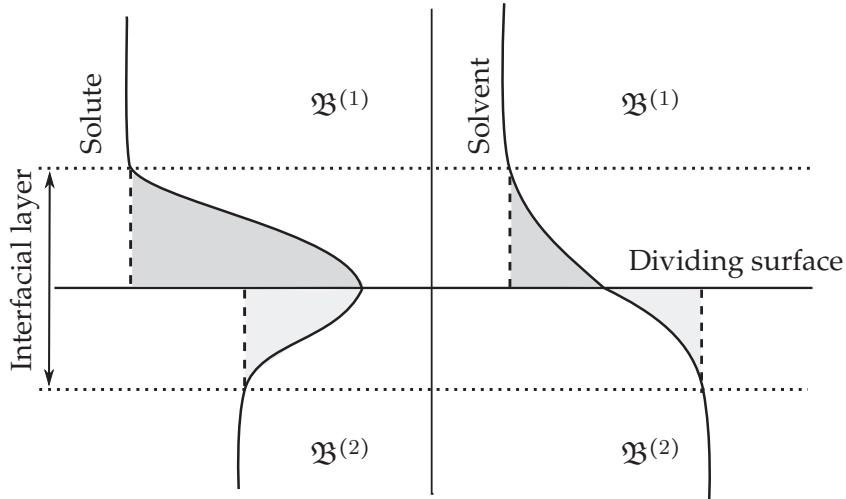


Figure 2.2: Surface excess concentration in a two-component system according to Mitropoulos (2008). The concentration profile is given as a function of distance normal to the phase boundary. The surface excess is the sum of shaded areas above and below of the dividing surface. Usually, the dividing surface is chosen as the zero surface excess of the solvent.

- the bulk and surface production densities, $\pi^{(i)}$ (in the bulk phases $\mathfrak{B}^{(i)}$, $i = 1, 2$) and $\pi^{(s)}$ on the phase interface, respectively,
- as well as the bulk and surface supply rate densities $\zeta^{(i)}$ (in the bulk phases $\mathfrak{B}^{(i)}$, $i = 1, 2$) and $\zeta^{(s)}$, on the interface, respectively.

Using these densities, one immediately obtains

$$P = \sum_{i=1}^2 \int_{\mathfrak{B}^{(i)}} \pi^{(i)} dv + \int_{\mathfrak{S}} \pi^{(s)} da \quad (2.3)$$

$$S = \sum_{i=1}^2 \int_{\mathfrak{B}^{(i)}} \zeta^{(i)} dv + \int_{\mathfrak{S}} \zeta^{(s)} da. \quad (2.4)$$

With respect to the non-convective fluxes, one assumes that the surface flux vector $\phi_C^{(s)}$ per unit length at the curve \mathfrak{C} depends on the coordinate x^c of \mathfrak{C} , the time t and the line normal s and has the form

$$\phi_C^{(s)} = \phi_C^{(s)}(x^c, t, s) = -\phi^{(s)} \cdot s. \quad (2.5)$$

The equality on the right hand side results from the Cauchy lemma for the line flux density, which implies a linear dependence if the line flux density $\phi_C^{(s)}$ depends on the normal at the line s . In sum,

$$F = - \sum_{i=1}^2 \int_{\partial \mathfrak{B}^{(i)}} \phi^{(i)} \cdot \mathbf{n} da - \int_{\mathfrak{C}} \phi^{(s)} \cdot \mathbf{s} dl. \quad (2.6)$$

As the partial volume $\mathfrak{B}^{(i)}$ is enclosed by the set $\partial\mathfrak{B}^{(i)} \cup \mathfrak{S}$, Gauss' divergence theorem can be applied to the surface density integrals in identity (2.6), i.e.

$$\int_{\partial\mathfrak{B}^{(i)}} \boldsymbol{\phi}^{(i)} \cdot \mathbf{n} \, da = \int_{\mathfrak{B}^{(i)}} \nabla \cdot \boldsymbol{\phi}^{(i)} \, dv - \int_{\mathfrak{S}} \boldsymbol{\phi}^{(i)} \cdot \mathbf{n}^{(s)} \, da, \quad i = 1, 2.$$

Inserting density integrals (2.3), (2.4) and (2.6) into equation (2.1) yields a mass balance statement in a setting with two phases in integral form:

$$\begin{aligned} & \sum_{i=1}^2 \frac{d}{dt} \int_{\mathfrak{B}^{(i)}(t)} \gamma^{(i)} \, dv + \frac{d}{dt} \int_{\mathfrak{S}} \gamma^{(s)} \, da \\ &= \sum_{i=1}^2 \int_{\mathfrak{B}^{(i)}} (\pi^{(i)} + \zeta^{(i)} - \nabla \cdot \boldsymbol{\phi}^{(i)}) \, dv \\ &+ \int_{\mathfrak{S}} (\pi^{(s)} + \zeta^{(s)}) \, da + \sum_{i=1}^2 \int_{\mathfrak{S}} \boldsymbol{\phi}^{(i)} \cdot \mathbf{n}^{(s)} \, da - \int_{\mathfrak{C}} \boldsymbol{\phi}^{(s)} \cdot \mathbf{s} \, dl. \end{aligned} \quad (2.7)$$

2.1.2 The Geometric Surface

With respect to the subsequent considerations, the notions of a parametric surface representation and of surface differentials will be needed. An evolving surface that is oriented by the normal field $\mathbf{n}^{(s)}$ can be represented by a local mapping $\mathbf{x}_i^{(s)} = \hat{\mathbf{x}}_i^{(s)}(\boldsymbol{\xi}^{(s)}, t)$, $i = 1, \dots, D$, introducing a set of parameters $\boldsymbol{\xi}^{(s)} = (\xi_1^{(s)}, \xi_2^{(s)})$ in a three-dimensional setting, or a single parameter $\boldsymbol{\xi}^{(s)} = \xi^{(s)}$, in the two-dimensional case, which is denoted as a one-dimensional vector here. As one important property, the local velocity field of the interface is given by the local time derivative of this mapping,

$$\mathbf{w}^{(s)}(\mathbf{x}, t) = \left. \frac{\partial \hat{\mathbf{x}}^{(s)}}{\partial t} \right|_{\boldsymbol{\xi}^{(s)}}. \quad (2.8)$$

Furthermore, a curvilinear coordinate system can be introduced on the surface based on the parametric form. The partial derivatives of the local mapping define its tangential vectors \mathbf{f}_i , i.e.

$$\mathbf{f}_i(\boldsymbol{\xi}^{(s)}, t) = \frac{\partial \hat{\mathbf{x}}^{(s)}}{\partial \xi_i^{(s)}}(\boldsymbol{\xi}^{(s)}, t), \quad i = 1, \dots, D-1,$$

which correspond to the tangent base vectors of a curvilinear coordinate system on the surface, provided that the mapping is sufficiently smooth. The normalization

$$\mathbf{e}_i(\boldsymbol{\xi}^{(s)}, t) = \frac{1}{\|\mathbf{f}_i\|} \mathbf{f}_i(\boldsymbol{\xi}^{(s)}, t), \quad i = 1, \dots, D-1$$

yields a set of orthonormal basis vectors with scale factors

$$h_i = \left\| \frac{\partial \hat{\mathbf{x}}^{(s)}}{\partial \xi_i^{(s)}} \right\|, \quad i = 1, \dots, D-1.$$